

CHAPTER 4

HYDROGENATION OF NATURAL RUBBER CATALYZED BY $\text{Ru}(\text{CH}=\text{CH}(\text{Ph}))\text{Cl}(\text{CO})(\text{PCy}_3)_2$

Natural rubber (NR) is harvested from the latex of the Brazilian rubber tree, *Hevea brasiliensis*. Natural rubber is comprised of polyisoprene, of almost 100% *cis*-configuration, and small amounts of abnormal groups such as aldehyde and epoxide. The non-aqueous components of latex are mixtures of 94% rubber hydrocarbon. The other non-rubber components include protein, lipids and carbohydrates (Eng et al., 1993). Since natural rubber cannot have its natural polymerization process tailored like that of the synthetic rubber industry, chemical modification is a useful postprocess for an alteration of the polymer composition and improvements in certain physical and chemical properties of unsaturated elastomers. Hydrogenation is a simple method for polymer modification that reduces the degree of C=C unsaturation present in the polymer which allows for greater stability against thermal, oxidative, and radiation-induced degradation. Singha et al. (1997b: 1647-1652) reported the quantitative hydrogenation of NR using $\text{RhCl}(\text{PPh}_3)_3$ as catalyst at high catalyst loading and long reaction time (> 20 h). The reaction kinetics of NR hydrogenation followed first order kinetics in residual double bonds. Hydrogenated natural rubber (HNR) is a plastic elastic waxy solid, which has found use due to its insulation properties, and potential for use in adhesives (Bhowmick A. K., and Stephens, H. L., 1988).

$\text{Ru}(\text{CH}=\text{CH}(\text{Ph}))\text{Cl}(\text{CO})(\text{PCy}_3)_2$ complexes have been reported to be efficient catalysts for hydrogenation of synthetic polyisoprene. However, hydrogenation of natural rubber is a rather difficult due to the non-rubber components in natural rubber. In this chapter, the hydrogenation of natural rubber (STR 5L) was carried out in the presence of $\text{Ru}(\text{CH}=\text{CH}(\text{Ph}))\text{Cl}(\text{CO})(\text{PCy}_3)_2$ as catalyst. The effect of catalyst level, concentration of polymer, hydrogen pressure, and temperature are studied. Since the catalytic activity of this catalyst for olefin hydrogenation has been found to increase by the addition of protic acid (Yi et al., 2000), this is also considered in the present study.

4.1 FTIR and NMR Spectroscopic Characterization

The typical IR spectra of natural rubber (NR) and its completely hydrogenated product (HNR) are depicted in Figure 4.1. The absence of the characteristic bands for the C=C unsaturation, i.e. at 1663 (C=C stretching) and 836 cm^{-1} (trisubstituted olefinic C-H bending) and the formation of strong band at 736 cm^{-1} due to $-(\text{CH}_2)_3-$ groups confirmed essential quantitative hydrogenation.

The degree of hydrogenation of the hydrogenated elastomer can be determined by $^1\text{H-NMR}$. The $^1\text{H-NMR}$ spectra for the parent NR and the hydrogenated NR (> 99% completion) are displayed in Figure 4.2. Upon hydrogenation, peaks at 1.7, 2.2 and 5.2 ppm which are assigned to $-\text{CH}_3$, $-\text{CH}_2-$, and $=\text{CH}$ groups, respectively disappeared and new peaks appeared at 0.8 and 1.1 – 1.8 ppm, attributed to saturated $-\text{CH}_3$ -, $-\text{CH}_2-$ groups.

4.2 Effect of Addition of Various Acids on the Natural Rubber Hydrogenation

Quantitative hydrogenation of NR using $\text{Ru}(\text{CH}=\text{CH}(\text{Ph}))\text{Cl}(\text{CO})(\text{PCy}_3)_2$ in chlorobenzene could be achieved at a catalyst concentration of 200 μM , 160°C, 40.3 bar hydrogen pressure, within 21 h as shown in Table 4.1, Entry 1. This result is generally much slower than the rate of CPIP hydrogenation in chlorobenzene catalyzed by Ru complexes under the same condition. This may be due to the high molecular weight of rubber and impurities in natural rubber. Effort has been made to increase the catalyst activity toward the hydrogenation reaction, the effect of acid addition on the reaction rate has been explored. It is evident that acid promotes the hydrogenation of synthetic polyisoprene (Section 3.3.9). The effect of added various acids on the hydrogenation of NR using $\text{Ru}(\text{CH}=\text{CH}(\text{Ph}))\text{Cl}(\text{CO})(\text{PCy}_3)_2$ are summarized in Table 4.1, Entry 2 - 4. Both concentrations of catalyst and acid were kept constant for this study. It is evident that the hydrogenation rate of NR using $\text{Ru}(\text{CH}=\text{CH}(\text{Ph}))\text{Cl}(\text{CO})(\text{PCy}_3)_2$ in presence of a small amount of added acid is greatly enhanced compared to that for NR using Ru complexes without added acid. *p*-toluenesulfonic acid (*p*-TsOH) was found to be the most efficient acid-promoter for hydrogenation of NR since the sulfonic acid is more acidic than the selected carboxylic acids. This suggests that the strong acid can accelerate the activity of Ru complexes more than weak acid in the order: *p*-TsOH > 3-chloropropionic acid > succinic acid.

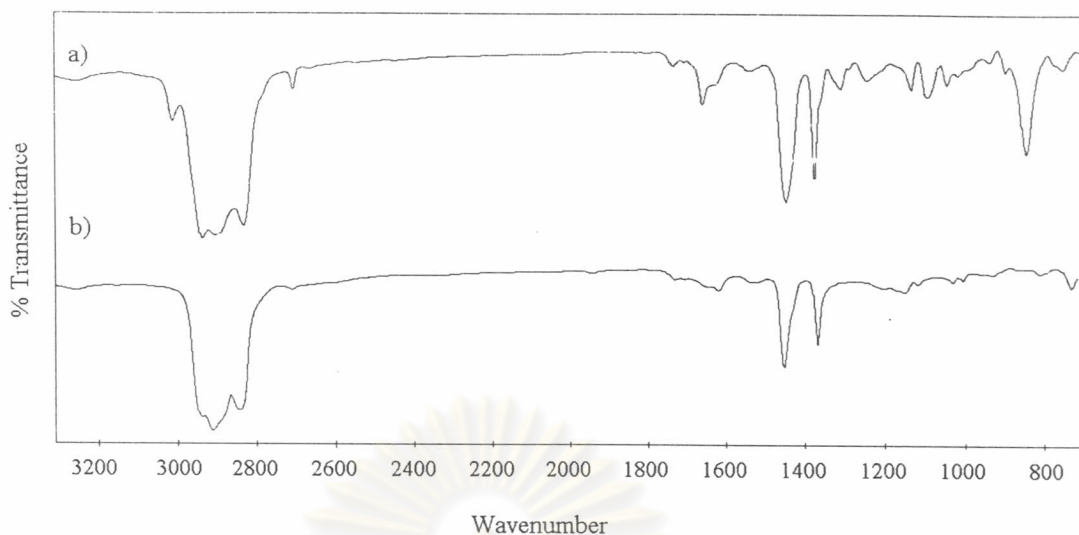


Figure 4.1: FTIR spectra of (a) NR, (b) HNR (> 99% hydrogenation), $[\text{Ru}] = 200 \mu\text{M}$; $[\text{C}=\text{C}] = 260 \text{ mM}$; $P_{\text{H}_2} = 40.3 \text{ bar}$; $T = 140^\circ\text{C}$; $[\text{p-TsOH}] = 8.8 \text{ equiv}$.
 $[\text{p-TsOH}]$ is defined as $[\text{acid}]/[\text{Ru}]$

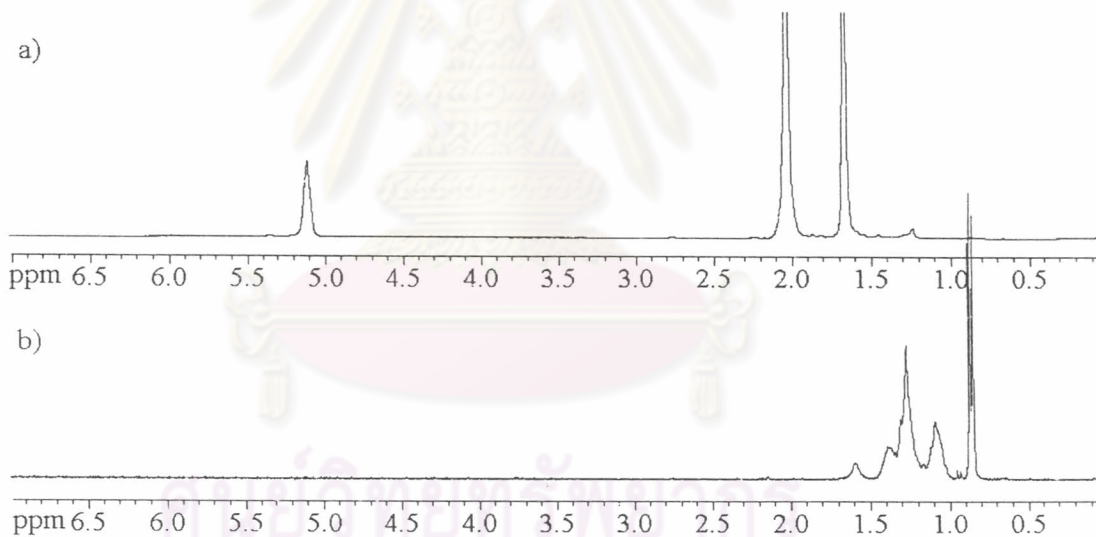


Figure 4.2: $^1\text{H-NMR}$ spectra of (a) NR, (b) HNR (>99% hydrogenation), $[\text{Ru}] = 200 \mu\text{M}$; $[\text{C}=\text{C}] = 260 \text{ mM}$; $P_{\text{H}_2} = 40.3 \text{ bar}$; $T = 160^\circ\text{C}$. $[\text{p-TsOH}] = 8.8 \text{ equiv}$.

Table 4.1: Effect of Addition of Various Acid on Natural Rubber Hydrogenation

Entry	Acid	Equivalents of added acid	% Hydrogenation	Time (h)
1	-	0.0	98.7	21
2	succinic acid	7.0	80.0	4
3	3-chloropropionic acid	7.7	97.7	4
4	<i>p</i> -toluenesulfonic acid	4.4	99.2	4

Conditions: T = 160°C; P_{H₂} = 40.3 bar; [C=C] = 260 mM; [Ru] = 200 μM in 150 ml chlorobenzene

Table 4.2: Effect of *p*-TsOH on the Hydrogenation of Natural Rubber

Entry	Treatment	Equivalents of added acid	Equivalents of added acid	% hydrogenation	Time (h)	Gel (%)
1	-	0.0	0.16	74.9	2.1	12.2 ^a
2	recoagulated rubber	0.0	0.17	63.2	1.5	55.5 ^a
3	dissolved rubber with acid	0.0	0.23	75.3	1.6	16.5 ^a
4	add acid in catalyst bucket	4.4	0.58	93.5	1.5	-
5	add acid in catalyst bucket	8.8	1.19	97.5	0.9	23.9 ^b
6	add acid in rubber solution	8.8	0.83	98.0	1.6	-

Condition: P_{H₂} = 40.3 bar; T = 160°C; [Ru] = 200 μM; [C=C] = 260 mM in 150 ml chlorobenzene

^a measured before hydrogenation

^b measured after hydrogenation

4.3 Initial Study in the Gas Uptake Apparatus

In an attempt to understand the effect of acid on the hydrogenation of NR in the presence of Ru complexes, a number of experiments were carried out using the gas uptake apparatus, with added *p*-TsOH as shown in Table 4.2. To investigate the effect of purifying the polymer before hydrogenation, rubber was dissolved in chlorobenzene, and then the solution was precipitated in ethanol (Entry 2). The sample was dried under vacuum for a week to remove trapped solvent. The purified sample was re-dissolved in chlorobenzene and hydrogenated under the base conditions ($[Ru] = 200 \mu M$, $[C=C] = 200 \text{ mM}$, $P_{H_2} = 40.3 \text{ bar}$, $T = 160^\circ C$). It can be seen that the hydrogenation rate is similar to the normal base condition run. Moreover, the sample after re-coagulation formed crosslinks during the drying process for unpurified rubber (Entry 1). Entry 3 shows the result of NR hydrogenation at the base conditions ($[Ru] = 200 \mu M$, $[C=C] = 200 \text{ mM}$, $P_{H_2} = 40.3 \text{ bar}$, $T = 160^\circ C$) after the rubber was dissolved with a small amount of added *p*-TsOH and separated from solution, dried under vacuum and dissolved again in chlorobenzene. The slight increase in hydrogenation rate trends to suggest that the acid may neutralize the impurities in the rubber. The presence of protein, evidence by the characteristic bands of N-H stretching at 3280 cm^{-1} , $-(NH)C=O$ at 1650 cm^{-1} and N-H bending at 1540 cm^{-1} in the FTIR spectrum (Figure 4.1), suggested that acid cannot remove protein in NR. However, the acid still may interact with the nitrogenous substances to prevent them from complexing with Ru. The hydrogenation of NR using Ru catalyst with added *p*-TsOH in the catalyst bucket was displayed in Entry 4-5. Although the mechanism of the effect of acid during the hydrogenation is not clear, the additive did affect the activity of catalyst on hydrogenation as shown by the increase in rate constant. Yi et al. (2000) proposed that the effect of acid-promoter on alkene hydrogenation can be explained by the acid induced selective dissociation of phosphine ligand on the ruthenium-hydride complex, $(RuHCl(CO)(PCy_3)_2)$. An increase of acid amount tended to increase the hydrogenation rate. In addition, the rate of reaction was found to be considerably lower if acid was added in the rubber solution (Entry 6), compared to the reaction in the presence of acid in the catalyst bucket (Entry 5). Therefore, the acid could play in a number of important roles such as a scavenger of the rubber contaminants, and a promoter for the selective entrapment of the phosphine ligand.

From these initial experimental results, adding 8.8 equivalents of *p*-TsOH in the catalyst bucket was deemed to be a preferred condition for examination of a detailed kinetic study of NR hydrogenation.

4.4 Kinetics of NR Hydrogenation using Ru(CH=CH(Ph))Cl(CO)(PCy₃)₂

A detailed kinetic study of the hydrogenation of NR in the presence of Ru(CH=CH(Ph))Cl(CO)(PCy₃)₂ and *p*-TsOH in chlorobenzene was investigated in an attempt to gain better understanding of the reaction mechanism. In Table 4.3, a summary of the results for a series of experiments showing the effect of the reaction variables on *k'* is provided. In all cases the reaction gave rise to typical first order plots up to high levels of conversion. Thus, the hydrogenation rate is proportional to the double bond concentration, according to

$$\frac{-d[C=C]}{dt} = k'[C=C] \quad (4.1)$$

where *k'* is the pseudo first order rate constant. First order rate constants for a variety of reaction conditions were obtained from straight-line first order plots (Figure 4.3) and are summarized in Table 4.3.

4.4.1 Effect of the Ruthenium Concentration

Two sets of experiments in which the ruthenium concentration was varied over the range of 30 to 200 μM at 160°C with 8.8 equivalent of *p*-TsOH concentration were performed to determine the influence of the catalyst concentration on the rate of hydrogenation. The first set kept the initial concentration of polymer at 260 mM under 40.3 bar hydrogen pressure and the second set of experiments used a polymer concentration of 130 mM. The pseudo first order rate constant, as a function of [Ru], at both levels of olefin concentration is linearly proportional to the total concentration of ruthenium complexes as illustrated in Figure 4.4. This agrees well with the investigation of synthetic *cis*-1,4-polyisoprene and NBR (Martin et al., 1997) hydrogenation using the analogous ruthenium system. The first order dependence on the catalyst concentration loading indicated that the concentration of the active complex is linearly proportional to the precursor loading. This suggests that the active complex is a mononuclear species.

Table 4.1: Summary of Kinetic Data from the Study of NR Hydrogenation Catalyzed by Ru(CH=CH(Ph))Cl(CO)(PCy₃)₂

Expt.	[Ru] (μM)	[C=C] ₀ (mM)	P _{H₂} ^a (bar)	<i>p</i> -TsOH (equiv.)	Temp (°C)	k' $\times 10^3$ (s ⁻¹)	% Hydrogenation	Time (h)
1	50	260	40.3	8.8	160	0.07	21.9	1.05
2	80	260	40.3	8.8	160	0.28	72.1	1.66
3	150	260	40.3	8.8	160	0.63	96.8	1.61
4	200	260	40.3	8.8	160	1.18	97.5	0.94
5	30	130	40.3	8.8	160	0.18	47.1	0.91
6	50	130	40.3	8.8	160	0.46	49.8	0.49
7	100	130	40.3	8.8	160	0.91	83.8	0.58
8	150	130	40.3	8.8	160	1.39	90.3	0.32
9	200	130	40.3	8.8	160	1.71	97.0	0.32
10	200	260	19.7	8.8	160	0.50	89.0	1.52
11	200	260	54.1	8.8	160	1.51	98.0	0.74
12	200	260	67.9	8.8	160	1.95	97.6	0.52
13	200	420	40.3	8.8	160	0.69	93.4	1.33
14	200	260	40.3	8.8	90	0.33	75.4	0.79
15	200	260	40.3	8.8	110	0.59	85.1	0.63
16	200	260	40.3	8.8	140	0.91	99.4	1.45
17	200	260	40.3	8.8	170	1.04	94.0	0.73
18	200	260	40.3	8.8	180	0.75	74.6	0.74
19	200	130	40.3	8.8	100	1.08	78.4	0.38
20	200	130	40.3	8.8	120	1.78	98.0	0.48
21	200	130	40.3	8.8	140	2.74	97.1	0.35
22	200	260	40.3	0	160	0.16	74.9	2.12
23	200	260	40.3	4.4	160	0.58	93.5	1.48
24	200	260	40.3	6.1	160	0.89	99.6	1.65
25	200	260	40.3	13.2	160	1.29	81.8	0.54

^a partial pressure of H₂, Solvent = chlorobenzene, Volume = 150 ml

It was noticed that the plots of NR hydrogenation show a positive intercept on the x-axis, whereas this behavior is not observed for CPIP hydrogenation. This can be explained that some portion of Ru catalyst was sacrificed with the impurities in the natural rubber. It appears that about 45 μM of the active catalyst was destroyed when the concentration of rubber was 260 mM, but at lower concentration of polymer (130 mM), a much smaller amount of catalyst was sacrificed. Therefore, increasing impurities as the concentration of natural rubber increases results in decreasing the amount of active catalyst for the hydrogenation reaction.

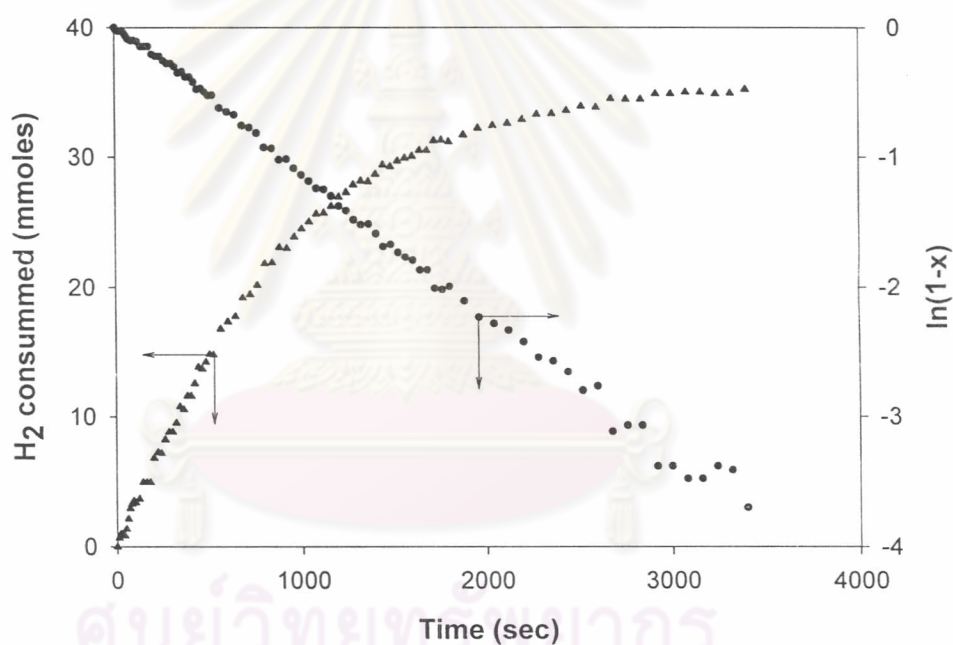


Figure 4.3: Hydrogen consumption plot for NR hydrogenation, $[\text{Ru}] = 200 \mu\text{M}$; $[\text{C}=\text{C}] = 260 \text{ mM}$; $[p\text{-TsOH}] = 8.8 \text{ equiv}$; $P_{\text{H}_2} = 40.3 \text{ bar}$; $T = 160^\circ\text{C}$ in 150 ml chlorobenzene.

4.4.2 Effect of Hydrogen Pressure

The influence of hydrogen pressure on the rate of hydrogenation was varied over the range of 19.7 - 67.9 bar at $[\text{Ru}] = 200 \mu\text{M}$, $[\text{C}=\text{C}] = 260 \text{ mM}$, $[\text{p-TsOH}] = 8.8$ equivalent and 160°C in chlorobenzene solvent. A first order rate dependence on hydrogen concentration tends to suggest that a single reaction mechanism is probably involved for the reaction of the unsaturation in polymer with hydrogen (Figure 4.5). If more than one process were involved, the relative contribution of these reactions should change as the hydrogen pressure changed, and thus the dependence might deviate from first order behavior. A similar observation was made from the H_2 univariate experiments of NBR (Martin, et al., 1997). This investigation illustrated the first order with respect to the experimental rate constant on hydrogen pressure that is characteristic of this ruthenium catalyst. In contrast, the extent of hydrogenation of NR in the presence of $\text{RhCl}(\text{PPh}_3)_3$ increased with an increase in hydrogen pressure at low hydrogen concentration and leveled off at higher hydrogen concentration (Singha, et al., 1997b: 1647-1652). Gan et al. (1996) hydrogenated NR in hexane using nickel 2-ethylhexanoate in combination with triisobutylaluminum. The rate of reaction increased with a higher initial hydrogen pressure.

4.4.3 Effect of Double Bond Concentration

The dependence of the initial hydrogenation rate on the carbon - carbon double bond concentration was studied over the range of 130 – 420 mM at 160°C with concentration of catalyst $200 \mu\text{M}$, 40.3 bar hydrogen pressure, and 8.8 equivalent acid concentration. A plot of initial rate versus initial carbon – carbon unsaturation is shown in Figure 4.6. As mentioned above, the hydrogenation profiles that followed pseudo first order with respect to $[\text{C}=\text{C}]$, by definition, should be independent of the amount of olefin charged to the reactor. The hydrogenation rate constant of NR; however, decreased with increasing the polymer concentration. The studies of synthetic polyisoprene hydrogenation catalyzed by $\text{Ru}(\text{CH}=\text{CH}(\text{Ph}))\text{Cl}(\text{CO})(\text{PCy}_3)_3$ have shown that the activity of Ru catalyst is independent of the amount of olefin charged to the system as shown in Figure 4.6. A recent study of the CPIP hydrogenation in the presence of analogous osmium system, $\text{OsHCl}(\text{CO})(\text{O}_2)(\text{PCy}_3)_2$ revealed that the additional of hexylamine into the system decreased the catalyst activity significantly (Hinchiranan et al.). Therefore, the inverse behavior of $[\text{C}=\text{C}]$ on

increasing $[C=C]$ is attributed to the effect of impurities within NR on decreasing the catalyst activity.

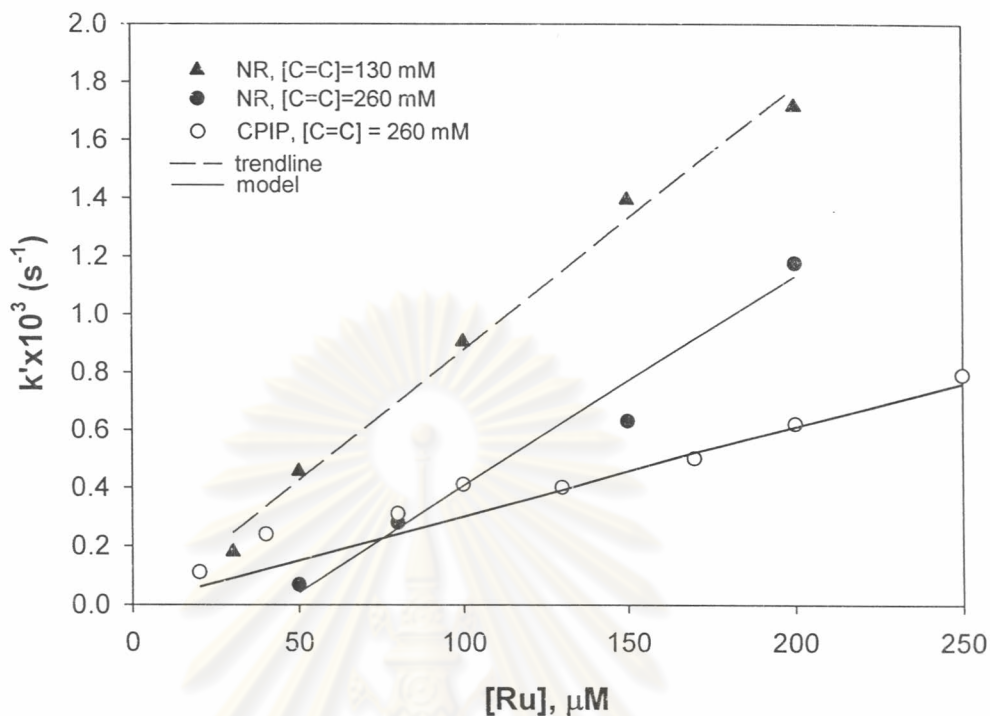


Figure 4.4: Effect of $[\text{Ru}]$ on rate constant,
For NR: $P_{\text{H}_2} = 40.3$ bar; $T = 160^\circ\text{C}$; $[p\text{-TsOH}] = 8.8$ equiv.
For CPIP: $P_{\text{H}_2} = 40.3$ bar; $T = 160^\circ\text{C}$.

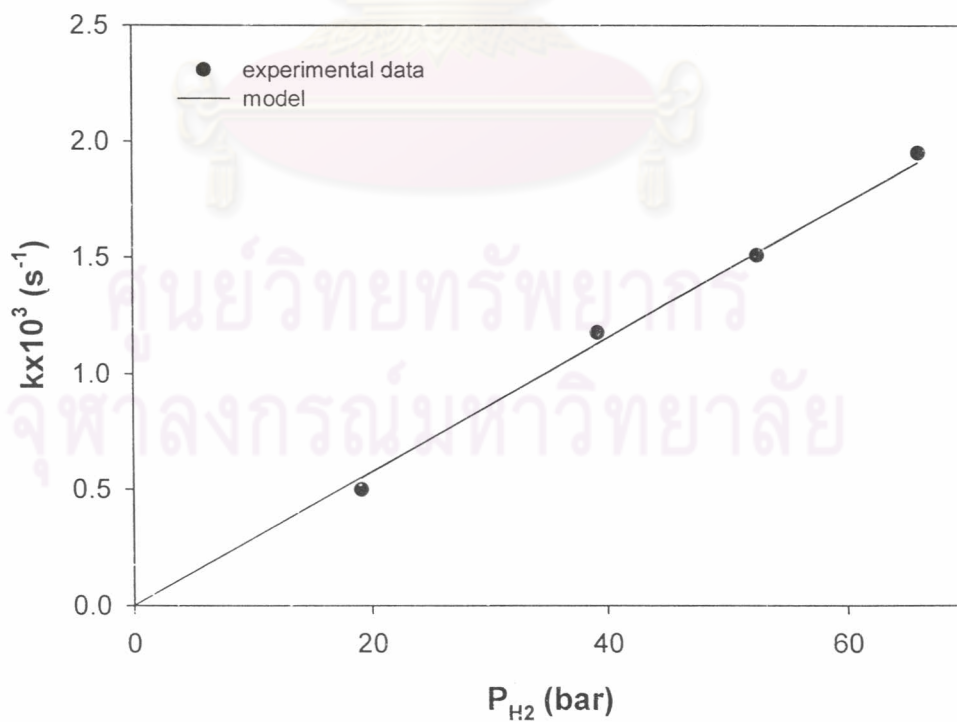


Figure 4.5: Effect of P_{H_2} on the rate constant,
 $[C=C] = 260$ mM; $[\text{Ru}] = 200$ μM ; $T = 160^\circ\text{C}$; $[p\text{-TsOH}] = 8.8$ equiv.

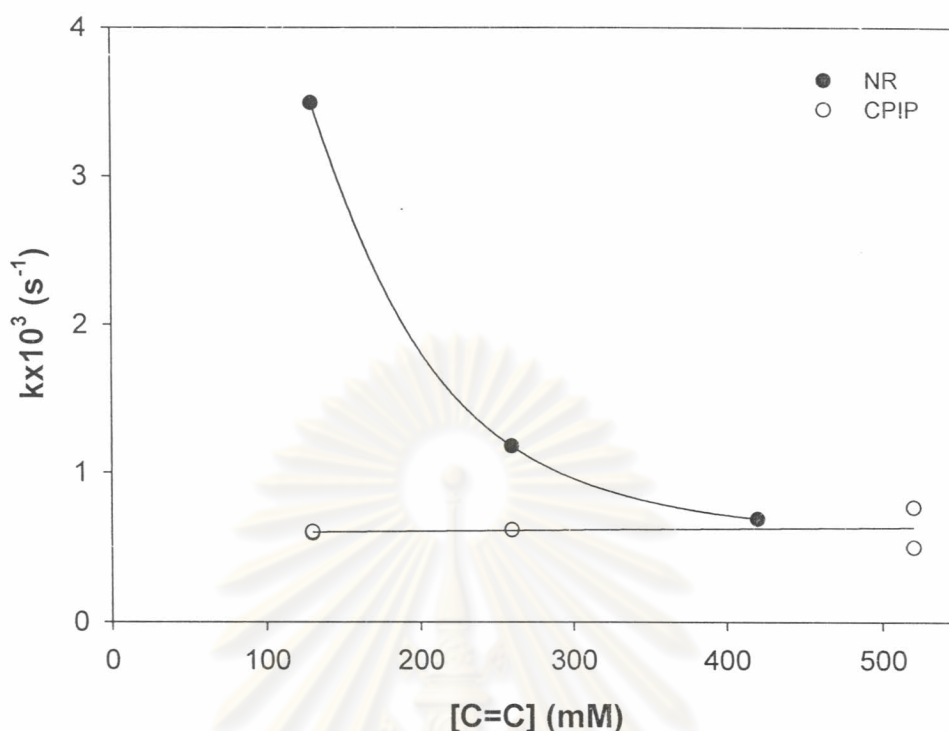


Figure 4.6: Effect of [C=C] on the rate constant,
 For NR: [Ru] = 200 μ M; P_{H_2} = 40.3 bar; T = 160°C; [*p*-TsOH] = 8.8 equiv.
 For CPIP: [Ru] = 200 μ M; P_{H_2} = 40.3 bar; T = 160°C.

4.4.4 Effect of Added Tricyclohexylphosphine

The dependence of the initial hydrogenation rate on the addition of tricyclohexylphosphine (PCy_3) was investigated to understand the function of the PCy_3 ligand on the role of the active Ru species in the catalytic mechanism. The values of the experimental rate constant along with the concentration of added PCy_3 are presented in Figure 4.7. Amounts ranging from 0.2 to 1.5 equivalents (1.5 times the number of moles of catalyst in the reactor) of tricyclohexylphosphine were used. It is evident that adding tricyclohexylphosphine retards the potential activity of the ruthenium complexes for hydrogenation. It may be explained by two mechanisms; the competitive coordination of PCy_3 with the active catalyst (Equation 4.2) or the inhibition of phosphine dissociation from ruthenium hydride species (Equation 4.3).



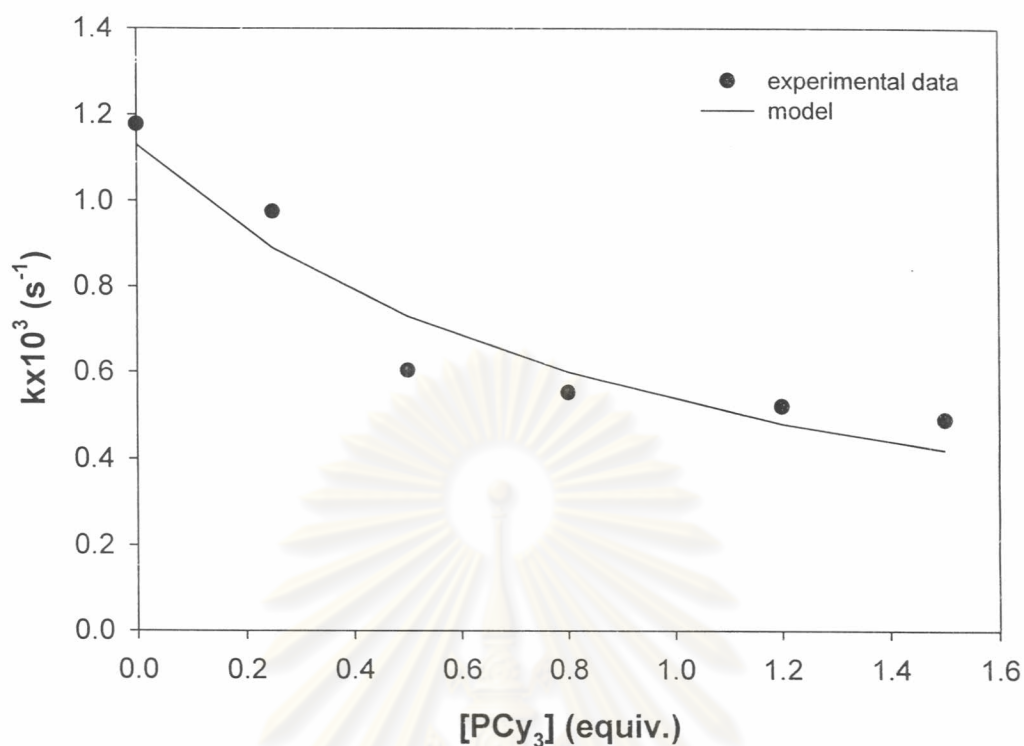


Figure 4.7: Effect of added PCy₃ on the rate constant, [C=C] = 260 mM; [Ru] = 200 μM; P_{H₂} = 40.3 bar; T = 160°C, [p-TsOH] = 8.8 equiv.

4.4.5 Effect of Temperature

The dependence of the hydrogenation rate on temperature was examined for 2 sets of experiments, over the range of 100 to 160°C for 130 mM of initial polymer concentration and 90 to 180°C for 260 mM of initial polymer concentration at the base condition. Figure 4.8 depicts temperature influence on hydrogenation rate constant. The results show that the temperature increase resulted in increasing the hydrogenation rate. However, the influence of temperature continued to decline with increasing temperature above 160°C. These results would seem to suggest that at higher temperature, the impurities in NR destroy more of the active catalyst. In other words, there may be 2 types of NR impurities, the primary one is easy to interact with the active catalysts whereas the secondary impurities is activated at high temperature i.e. higher than 160°C. Thus, the high amount of inactive catalysts at high temperature results in slow hydrogenation rate. Our previous studies on *cis*-1,4-polyisoprene hydrogenation showed that the rate constant increased as temperature was increased

over the range of 130 to 180°C. It can be concluded therefore that the ruthenium catalyst was not decomposed at temperature of 160 – 180°C.

The Arrhenius plot illustrated the temperature influence on the rate of hydrogenation as provided in Figure 4.9a. The apparent activation energies of 25.3 kJ/mol for 130 mM of polymer concentration over the temperature range of 100 – 160°C and 23.3 kJ/mol for 260 mM of olefin concentration over the temperature range of 90 – 160 °C was derived. These approximations show that increasing amount of polymer decreased the apparent activation energy. This is similar to a value of 29.1 kJ/mol observed for hydrogenation of NR using $\text{RhCl}(\text{PPh}_3)_3$ (Singha et al., 1997b: 1647-1652) and 26.0 kJ/mol reported for hydrogenation of NR in the presence of using nickel 2-ethylhexanoate and triisobutylaluminum (Gan et al., 1996). Although it is not totally understood the reason of the low value of apparent activation energy, it is believed that there is effect of active catalyst diffusion into the polymer particle due to the high viscosity of polymer. It is evident that the apparent activation energy of hydrogenation of synthetic CPIP which has lower molecular weight ($M_w = 800,000$) than that of NR ($M_w > 1,000,000$) is estimated to be 51.1 kJ/mol.

The Eyring equation was used to estimate the apparent activation enthalpy and entropy for the reactions. Figure 4.9b is the Eyring plot from the temperature dependence data. The enthalpy of activation was 20.0 kJ/mol and 21.9 kJ/mol and the entropy of activation was -137.5 J/mol K and -150.8 J/mol.K for 260 mM and 130 mM of polymer concentration, respectively.

ศูนย์วิทยทรัพยากร
จุฬาลงกรณ์มหาวิทยาลัย

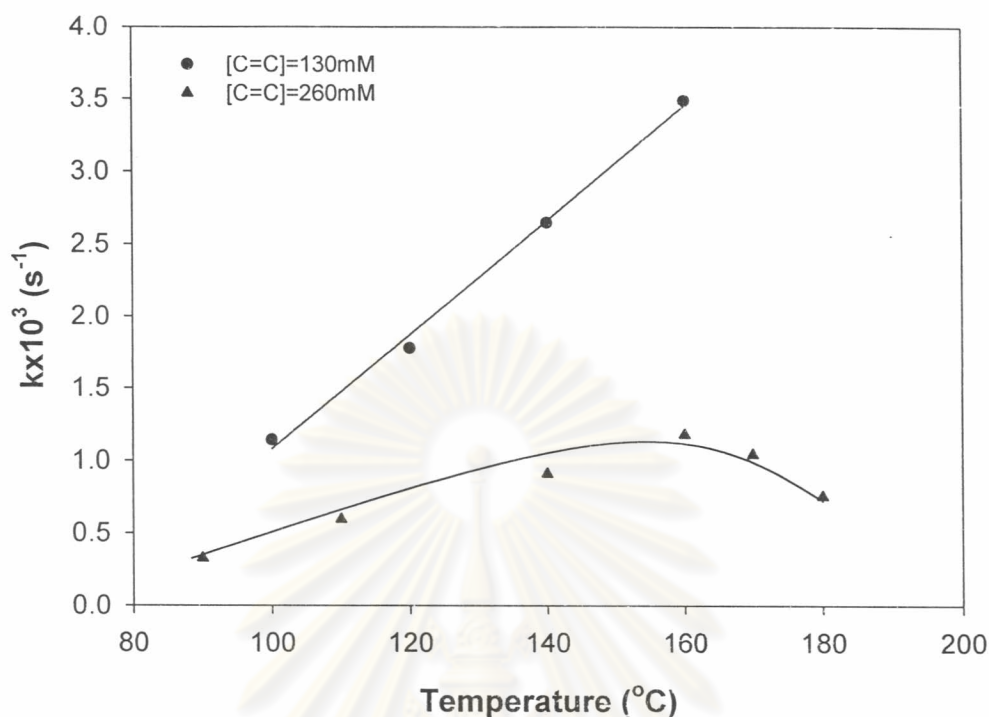


Figure 4.8: Effect of temperature on the rate constant, $P_{H_2} = 40.3$ bar; $[Ru] = 200 \mu M$; $[p\text{-TsOH}] = 8.8$ equiv.

4.4.6 Effect of Acid Concentration

The activity of ruthenium hydride catalyst is recognized to be dependent on the amount of acid addition as mention above. Figure 4.10 shows the effect of the concentration of acid on hydrogenation rate. As little as 4.4 mole equivalents (4.4 times the number of moles of catalyst in the reactor) of acid added to the system had significant effect on the catalyst activity. This result is similar to the observation of CPIP hydrogenation (Section 3.3.9). The increase in concentration of acid led to an increase in the rate of hydrogenation reaction. Although the mechanism of additive on the impurities in NR during the hydrogenation process is not clearly understood, the effectiveness of this additive in preventing the poisoning of Ru-based catalysts was very significant.

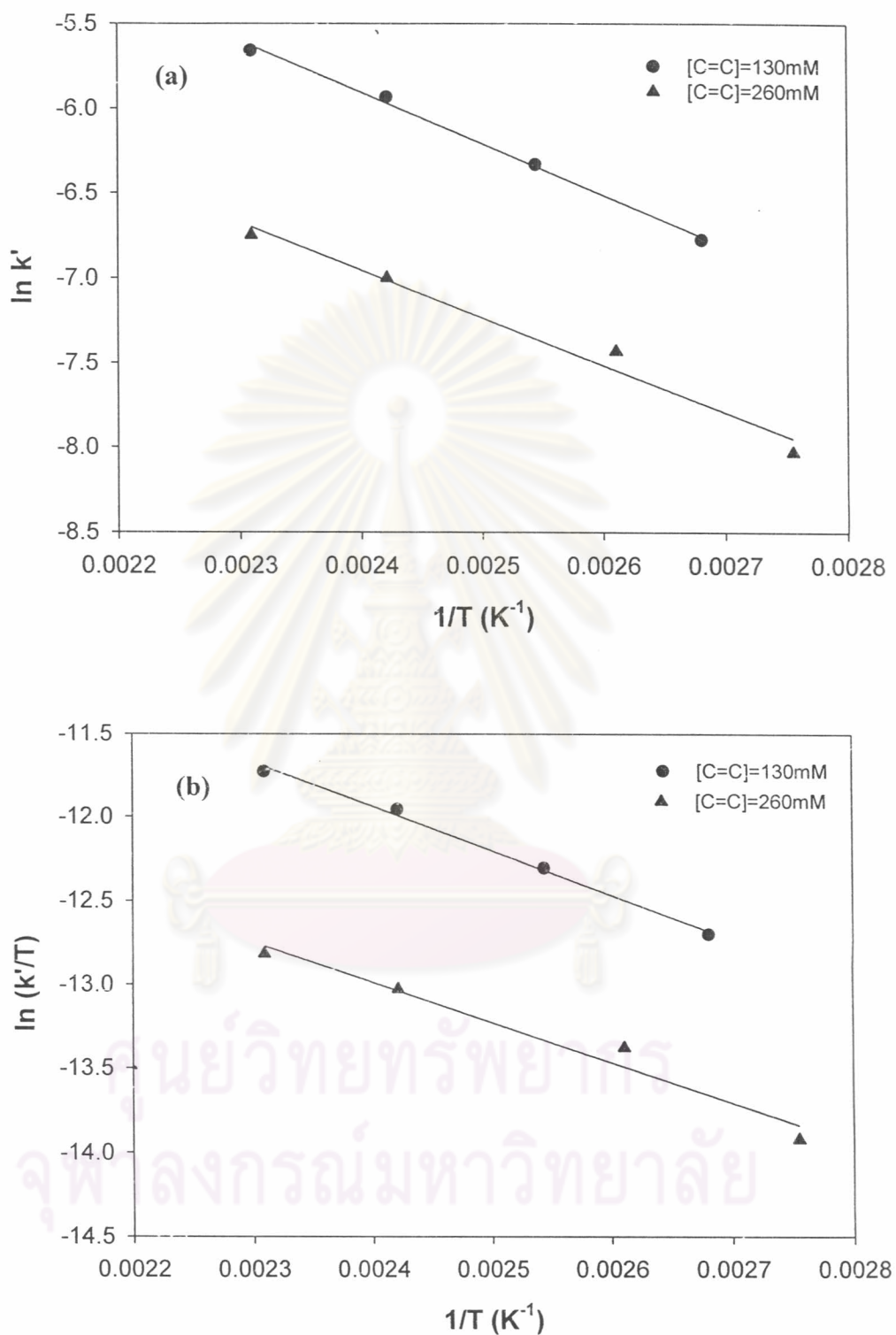


Figure 4.9: (a) Arrhenius plot, (b) Eyring plot for NR hydrogenation, $P_{H_2} = 40.3$ bar; $[Ru] = 200 \mu M$; $[p\text{-TsOH}] = 8.8$ equiv.

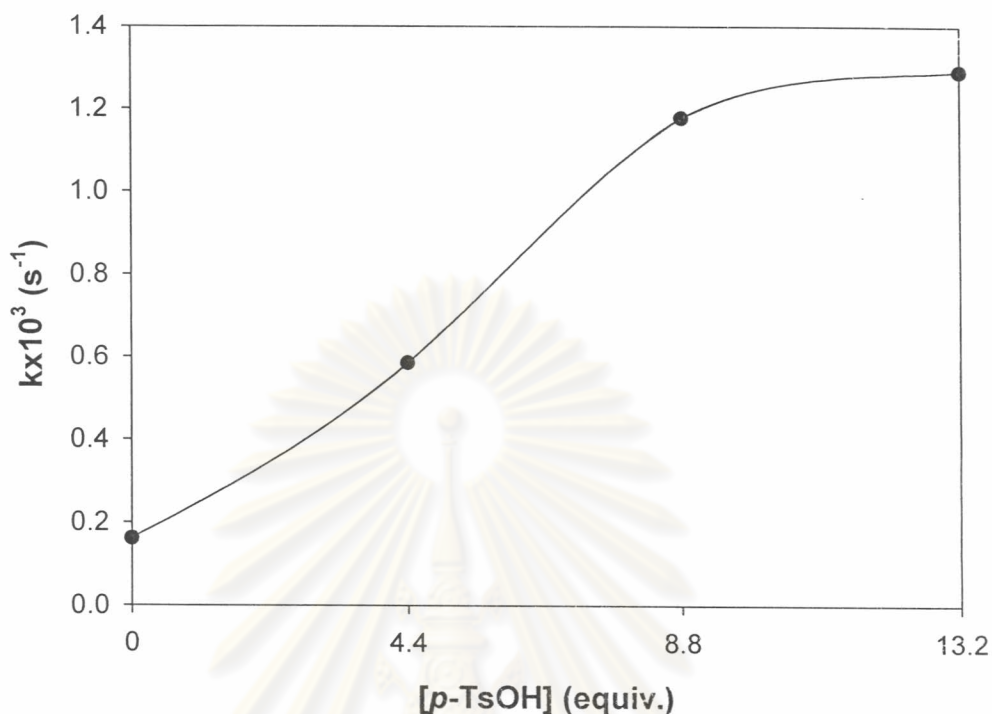


Figure 4.10. Effect of *p*-TsOH on the rate constant, $[\text{C}=\text{C}] = 260 \text{ mM}$; $P_{\text{H}_2} = 40.3 \text{ bar}$; $[\text{Ru}] = 200 \text{ }\mu\text{M}$; $T = 160^\circ\text{C}$

4.5 Polymer Chain Length Properties

Typically, gel permeation chromatography (GPC) analysis of NR shows a bimodal molecular weight distribution with high and low molecular weight peak. Figure 4.11 shows the gel permeation chromatograms for NR before hydrogenation and 98% hydrogenated NR at 160°C , $[\text{Ru}] = 200 \text{ }\mu\text{M}$, $P_{\text{H}_2} = 67.9 \text{ bar}$, $[\text{C}=\text{C}] = 260 \text{ mM}$, and 8.8 equiv. of *p*-TsOH, and Table 4.4 summarizes the molecular weight data. The nonhydrogenated rubber is partially insoluble in THF. However, its soluble part displayed a GPC chromatogram similar to its hydrogenated polymer and the molecular weight distribution was not changed significantly during hydrogenation. It can be noticed that hydrogenation of NR at high temperature (180°C) led to a significant decrease in the molecular weight of the hydrogenated rubber.

Table 4.4: Summary of GPC molecular weight data for NR and HNR

Polymer	Condition					Mn	Mw	Mw/Mn
	[C=C] (mM)	Temp (°C)	P _{H2} (bar)	[Ru] (μM)	<i>p</i> -TsOH (equiv.)			
NR	-	-	-	-	-	512000	974400	1.90
HNR	260	160	40.3	200	8.8	474600	939600	1.98
HNR	260	160	67.9	200	8.8	562200	962900	1.71
HNR	260	140	40.3	200	8.8	538600	1094000	2.03
HNR	260	180	40.3	200	8.8	415700	752600	1.81

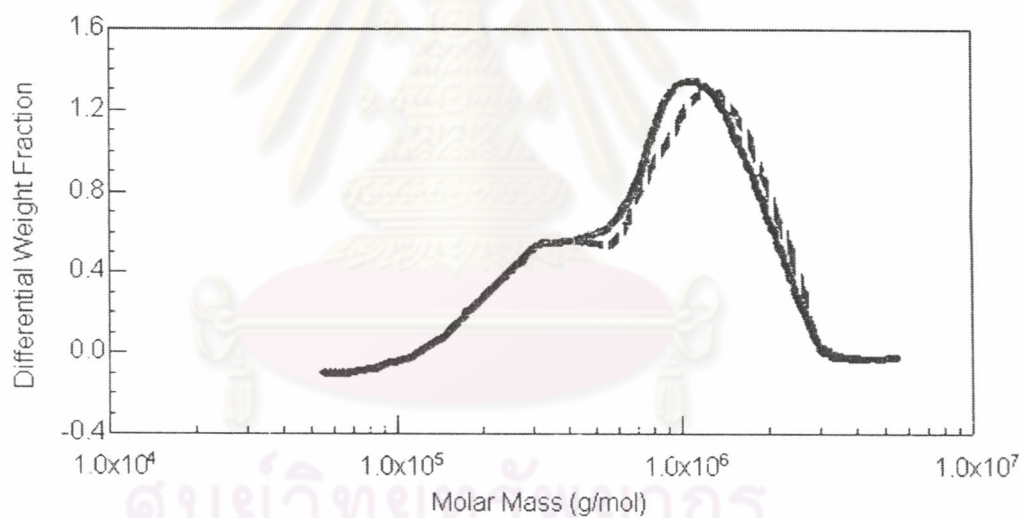


Figure 4.11: Gel permeation chromatograms of NR (-) and HNR (--), [Ru] = 200 μM; [C=C] = 260 mM; P_{H2} = 67.9 bar; T = 160°C; [*p*-TsOH] = 8.8 equiv.

4.6 Reaction Mechanism Consideration

A probable mechanism was proposed on the basis of results from the kinetic study and spectroscopic investigations. The experimental results showed that the reaction rate was first order with respect to the total ruthenium concentration and hydrogen pressure and inverse order on the concentration of added tricyclohexylphosphine over the range of conditions studied. The difficult element with the NR hydrogenation data is the effect of impurities in natural rubber. A plausible reaction mechanism as illustrated in Figure 4.12 is postulated for the hydrogenation of NR using $\text{Ru}(\text{CH}=\text{CH}(\text{Ph}))\text{Cl}(\text{CO})(\text{PCy}_3)_2$ as catalyst.

The reaction of $\text{Ru}(\text{CH}=\text{CH}(\text{Ph}))\text{Cl}(\text{CO})(\text{PCy}_3)_2$ with hydrogen to give the first hydride complex $\text{RuHCl}(\text{CO})(\text{PCy}_3)_2$ and ethyl benzene is rapidly formed. Then the phosphine ligand dissociates from hydride complex to form $\text{RuHCl}(\text{CO})(\text{PCy}_3)$. It was noticed that the catalytic cycle of NR is similar to that of hydrogenations of substrates lacking impurities (Section 3.5) except the impurities exhibit the inhibitory behavior. The presence of the impurities on completion of the hydrogenation is evident from the dramatic decrease of observed rate constant with adding the nitrogeneous substance in CPIP hydrogenation (Hinchiranan et al.). Therefore, the complex $\text{RuHCl}(\text{CO})(\text{PCy}_3)$ can either react with impurities within NR and/or coordinate with H_2 followed by coordination of carbon – carbon double bonds. The lack of a kinetic isotope effect observation implies that the rate-determining step involves the coordination of the catalyst with carbon – carbon double bonds within the polymer chain. Accordingly, NR hydrogenation could be governed by the rate expression

$$-\frac{d[\text{C}=\text{C}]}{dt} = k_{\text{rds}}[\text{Ru}(\text{H}_2)\text{HCl}(\text{CO})(\text{PCy}_3)][\text{C}=\text{C}] \quad (4.4)$$

Applying a steady-state assumption to each equilibrium reaction that leads to the formation of $[\text{Ru}(\text{H}_2)\text{HCl}(\text{CO})(\text{C}=\text{C})(\text{PCy}_3)]$ provides a means of relating the concentration of every species to the rate-determining step. The total amount of ruthenium $[\text{Ru}]_{\text{T}}$ used in each experiment may be accomplished using the mass balance of Equation 4.5.

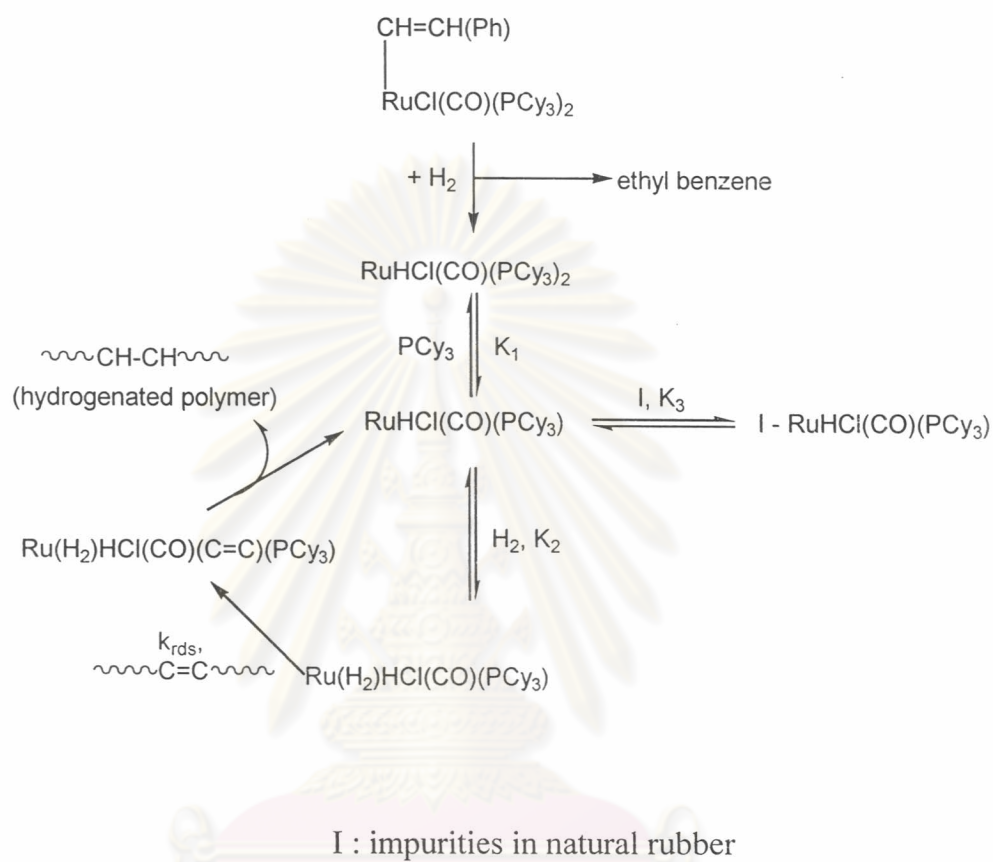


Figure 4.12: Proposed mechanism for hydrogenation of NR catalyzed by $\text{Ru}(\text{C}=\text{CH}(\text{Ph}))\text{Cl}(\text{CO})(\text{PCy}_3)_2$

$$[\text{Ru}]_T = [\text{RuHCl}(\text{CO})(\text{PCy}_3)_2] + [\text{RuHCl}(\text{CO})(\text{PCy}_3)] + [\text{I} - \text{RuHCl}(\text{CO})(\text{PCy}_3)] + [\text{Ru}(\text{H}_2)\text{HCl}(\text{CO})(\text{PCy}_3)] \quad (4.5)$$

A mass balance on ruthenium yields the concentration of the active center as a function of the total amount of ruthenium $[\text{Ru}]_T$ charged to the system and results in the rate expression

$$\begin{aligned} -\frac{d[\text{C}=\text{C}]}{dt} &= k_{\text{rds}}[\text{Ru}(\text{H}_2)\text{HCl}(\text{CO})(\text{PCy}_3)][\text{C}=\text{C}] \\ &= \frac{k_{\text{rds}}K_1K_2K_{\text{H}}P_{\text{H}_2}[\text{Ru}]_T[\text{C}=\text{C}]}{K_1 + K_1K_2K_{\text{H}}P_{\text{H}_2} + [\text{PCy}_3] + K_1K_3[\text{I}]} \end{aligned} \quad (4.6)$$

A comparison of Equation 4.6 with Equation 4.1 leads to the relation given by Equation 4.7.

$$k' = \frac{k_{\text{rds}}K_1K_2K_{\text{H}}P_{\text{H}_2}[\text{Ru}]_T}{K_1 + K_1K_2K_{\text{H}}P_{\text{H}_2} + [\text{PCy}_3] + K_1K_3[\text{I}]} \quad (4.7)$$

Since a rigorous first order dependence on hydrogen pressure, over the range of study, was observed the term of $K_1K_2K_{\text{H}}P_{\text{H}_2}$ in the denominator of Equation 4.7 is negligible. Thus, the model reduces to the following form:

$$k' = \frac{k_{\text{rds}}K_1K_2K_{\text{H}}P_{\text{H}_2}[\text{Ru}]_T}{K_1 + [\text{PCy}_3] + K_1K_3[\text{I}]} \quad (4.8)$$

Although the actual amount of impurities that has an effect of catalyst activity is unclear, it is evident that the system sacrificed amount of catalyst at a constant concentration of NR. The experimental results showed that about 45 μM of the ruthenium catalyst was destroyed when the concentration of NR was 260 mM in 150 ml chlorobenzene. Equation 4.9 provides a model for NR hydrogenation using 260 mM of polymer concentration, by assuming concentration of impurities is constant.

$$k' = \frac{k_4P_{\text{H}_2}([\text{Ru}]_T - C)}{K_5 + [\text{PCy}_3]} \quad (4.9)$$

The rate constant k_4 is a lumped constant containing the limiting reaction rate constant; k_{rds} , equilibrium constant; K_1 and K_2 , and the Henry's law constant for the solubility of hydrogen in chlorobenzene; K_H . Whereas the rate constant K_5 represents $K_1+K_1K_3[I]$ and C is correction factor which is assumed constant for each concentration of natural rubber.

A statistical analysis was undertaken to check the validity of the derived rate law. A summary of this analysis is shown in Table 4.5 and Table 4.6. The solid curves provided in Figure 4.4, 4.5 and 4.7 show how well the model predictions fit the observed experimental data. Actual model predictions of olefin conversion profile relative to the data from gas uptake are plotted in Figure 4.13. A plot of residual from the best fit versus k' (Figure 4.14) gave a random distribution confirming that the Equation 4.9 is valid model for hydrogenation of NR over the range of study.

Table 4.5: Model Parameter Estimates

Parameter	Asymptotic 95 %			
	Asymptotic		Confidence Interval	
	Estimate	Std. Error	Lower	Upper
$k_4, (\text{mM})^{-1} \text{s}^{-1} \text{bar}^{-1}$	3.24E-02	4.97E-03	2.12E-02	4.37E-02
$K_5, (\text{mM})^{-1} \text{bar}^{-1}$	1.80E-01	2.77E-02	1.17E-01	2.42E-01
$C, (\text{mM})$	4.46E-02	8.72E-03	2.49E-02	6.44E-02

Table 4.6: Model Analysis of Variance Results

Source	DF	Sum of Squares	Mean Square
Regression	3	10.270	3.424
Residual	9	0.058	6.472E-03
Uncorrected Total	12	10.329	
(Corrected Total)	11	3.191	

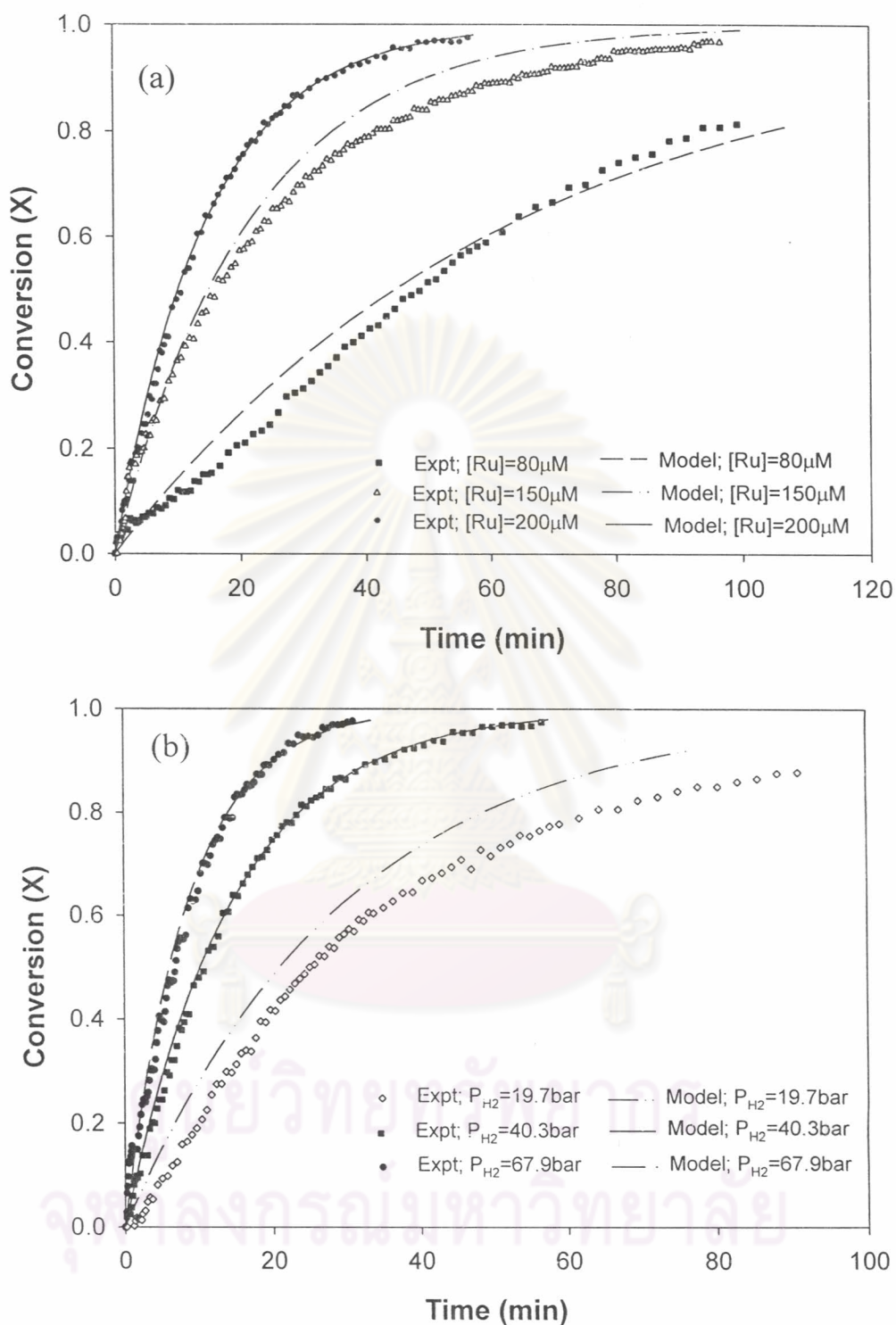


Figure 4.13: Comparison of the conversion profiles of experiment with model prediction.

(a) Conversion profile at various with Ru concentration, [C=C] = 260 mM; P_{H₂} = 40.3 bar; T = 160°C; [p-TsOH] = 8.8 equiv.

(b) Conversion profile at various hydrogen pressure, [C=C] = 260 mM; [Ru] = 200 μM; T = 160°C; [p-TsOH] = 8.8 equiv.

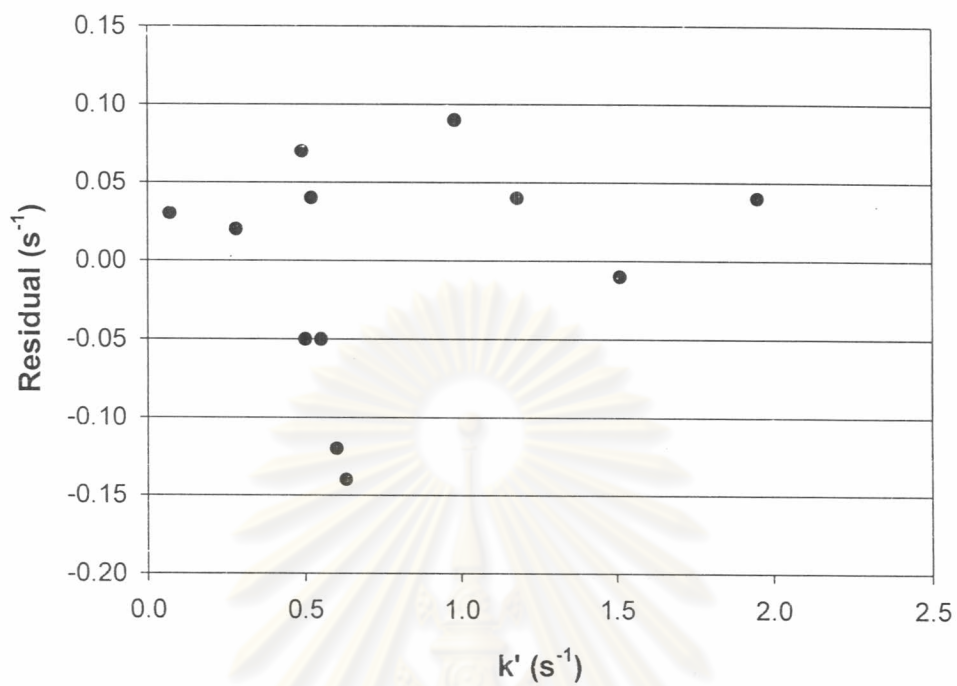


Figure 4.14: Residual plot from non-linear regression

ศูนย์วิทยทรัพยากร
จุฬาลงกรณ์มหาวิทยาลัย